PAPER

Check for updates

Electrochemical treatment in KOH improves carbon nanomaterial performance to multiple neurochemicals†

Samuel M. Hanser, [ID] Zijun Shao, He Zhao and B. Jill Venton [ID] *

Carbon-fiber microelectrodes (CFMEs) are primarily used to detect neurotransmitters *in vivo* with fast-scan cyclic voltammetry (FSCV) but other carbon nanomaterial electrodes are being developed. CFME sensitivity to dopamine is improved by applying a constant 1.5 V *vs.* Ag/AgCl for 3 minutes while dipped in 1 M KOH, which etches the surface and adds oxygen functional groups. However, KOH etching of other carbon nanomaterials and applications to other neurochemicals have not been investigated. Here, we explored KOH etching of CFMEs and carbon nanotube yarn microelectrodes (CNTYMEs) to characterize sensitivity to dopamine, epinephrine, norepinephrine, serotonin, and 3,4-dihydroxyphenylacetic acid (DOPAC). With CNTYMEs, the potential was applied in KOH for 1 minute because the electrode surface cracked with the longer time. KOH treatment increased electrode sensitivity to each cationic neurotransmitter roughly 2-fold for CFMEs, and 2- to 4-fold for CNTYMEs. KOH treatment decreased the background current of the CFMEs by etching the surface carbon; however, KOH-treatment increased the CNTYME background current because the potential separates individual nanotubes. For DOPAC, the current increase was smaller at CNTYMEs because it is anionic and was repelled by the negative holding potential and did not access the crevices. XPS and Raman spectroscopy showed that KOH treatment changed the CNTYME surface chemistry by increasing defect sites and adding oxide functional groups. KOH-treated CNTYMEs had less fouling to serotonin than normal CNTYMEs. Therefore, KOH treatment activates both CFMEs and CNTYMEs and could be used in biological measurements to increase the sensitivity and decrease fouling for neurochemical measurements.

Introduction

Carbon-fiber microelectrodes (CFMEs) have been the standard electrode used with fast-scan cyclic voltammetry (FSCV) for the real-time *in vivo* detection of electroactive chemicals.[1–4] They are an ideal material to be placed in tissue because of their biocompatibility, low cost, and small size.[5–7] Carbon fibers are a cylinder of flat graphene sheets and analytes often physically adsorb to the carbon surface before electrochemical detection. Oxygen surface functional groups on the CFME surface can facilitate better analyte adsorption.[8–12] To improve CFME performance, treatments have been developed, including laser, electrochemical, and flame etching.[13–15] Applying a constant 1.5 V potential difference *vs.* Ag/AgCl to a CFME for 3 minutes while dipped in 1 M KOH improved the electrode's perform-

Department of Chemistry, University of Virginia, Charlottesville, VA 22904, USA.
E-mail: bjv2n@virginia.edu
†Electronic supplementary information (ESI) available. See DOI: https://doi.org/10.1039/d3an01710a

ance in detecting dopamine.[16] This treatment creates surface defect sites, brakes graphitic carbon bonds which cleans the surface, and adds oxygen functional groups. However, that study only considered dopamine and CFMEs, and there has been little investigation into other analytes or types of carbon electrodes.

Carbon nanotube yarn microelectrodes (CNTYME) are a new type of carbon nanomaterial electrode made from a yarn of vertically-aligned carbon nanotubes.[17–20] CNTYMEs are made of graphene sheets that are rolled into a tube, and then those tubes are vertically-aligned and twisted together into a yarn.[17,21,22] They are disk electrodes because the yarn is polished to be flush with the glass casing, and they have high sensitivity, selectivity, and anti-fouling properties.[23,24] Also, CNTYMEs have a high temporal resolution and are frequency-independent in FSCV because they momentarily trap analytes between the individual CNTs.[18,25,26] Treatments used to activate CNTYME include electrochemical etching, plasma, laser, and antistatic gun treatments.[27–30] In particular, oxygen plasma etching changes the surface chemistry, but others such

as anti-static gun separate individual CNTs and increase the surface area; however, KOH treatment of CNTYMEs has not yet been explored.

Dopamine is an important electroactive neurotransmitter involved in motivation, movement, and reward.[31] Dopamine is an excellent test compound and is involved in many diseases in the brain, including Parkinson's disease and addiction.[31,32] Fewer studies have addressed electrode development for other electroactive neurotransmitters. Electroactive monoamine neurochemicals include catecholamines such as norepinephrine, which is involved in reward, and epinephrine, which is involved in sympathetic nervous system fight-or-flight response.[32,33] Serotonin is a widely studied indoleamine neurotransmitter because it is involved in many biological functions such as perception, mood, and cognition.[34] Dopamine (pK_a = 8.9), epinephrine (pK_a = 8.59), norepinephrine (pK_a = 8.58), and serotonin (pK_a = 9.41) all have a basic amino group which makes them all positively charged at pH = 7.4. 3,4-Dihydroxyphenylacetic acid (DOPAC, pK_a = 4.25) is an electroactive metabolite of dopamine and its carboxylic acid group makes it anionic at pH = 7.4. Studying a wider array of neurochemicals gives a better idea of how generalizable an electroactive treatment is to increase electrode sensitivity.

In this work, we examined how KOH treatment changes sensitivity of CFME and CNTYME to dopamine, epinephrine, norepinephrine, DOPAC, and serotonin. While both CFMEs and CNTYMEs have increased electrochemical responses, the background currents decreased on CFMEs and increased on CNTYMEs. The signals for dopamine, epinephrine, norepinephrine and serotonin all increased about 1.7-fold on a CFME and about 3-fold on a CNTYME. The signal for DOPAC increased by the same 1.7-fold on the CFME, but had a smaller increase than the cations on the porous CNTYME. Raman spectra and XPS showed that as the KOH treatment is applied for longer lengths of time, the number of surface defect sites and oxygen functional groups increased on the CNTYME. Thus, KOH treatment activates the surface of a CFME, even though it decreases the surface area, and it also activates the CNTYME while increasing its surface area by separating individual CNTs. The KOH treatment is fast, simple, and easy pretreatment for increasing sensitivity of multiple carbon electrodes for many neurochemicals.

Experimental

Chemicals

Dopamine was purchased from Acros Organics (Morris Plains, NJ), and epinephrine, norepinephrine, 3,4-dihydroxyphenylacetic acid (DOPAC), and serotonin were all purchased from Sigma Aldrich (Saint Louis, MO). A, 10 mM stock solution of each analyte was prepared in 0.1 M $HClO_4$. The stock solutions were then diluted in phosphate-buffered saline (PBS) (131.25 mM NaCl, 3.00 mM KCl, 10 mM NaH_2PO_4, 1.2 mM $MgCl_2$, 2.0 mM Na_2SO_4, and 1.2 mM $CaCl_2$, with pH adjusted to 7.4) to the desired concentrations for the working solution.

The working concentrations were typically 1 μM for DA, EP, NE, and 5HT, and 20 μM for DOPAC, but calibration curves were also produced to test electrodes at various relevant physiological concentrations. A 1 M KOH solution was prepared as the treatment solution.

Electrode fabrication

Carbon fiber microelectrodes were constructed using a vacuum to pull a T-650 carbon fiber (7 μm diameter, Cytec Engineering Materials, West Patterson, NJ) into a glass capillary. The capillary was then inserted into a vertical electrode puller (model PE-21, Narishige, Tokyo, Japan) to create two electrodes from one capillary. The carbon fiber was then cut to a length of approximately 20–30 μm past the end of the glass. The electrode was then sealed by dipping it in 80 °C Epon Resin 828 (Danbury, CT) with 14% (w/w) m-phenylenediamine (Acros Organics, Morris Plains, NJ) for 35 seconds, and then was cured in acetone for 5 seconds. The electrode was placed in a 100 °C oven for 2 hours, and then in a 150 °C oven overnight.

Carbon nanotube yarn microelectrodes were fabricated using 50 μm diameter carbon nanotube yarn (purchased from Nanoworld Lab, Department of Chemical and Environmental Engineering, University of Cincinnati). A glass capillary was pulled by a pipette puller, and the yarn was inserted into the opening at the tip. Isopropanol was applied to remove surface impurities before the electrode was epoxied with Epon Resin 828 and cured in a similar fashion to the CFME. The CNTYME was then polished at a 45° angle on a fine diamond abrasive plate (Sutter Instruments model BV-10, Novato, CA) so that the carbon is flush with the glass casing. The CNTYME was soaked in isopropanol for 5–10 minutes to remove impurities from fabrication.

Fast-scan cyclic voltammetry

FSCV experiments were performed on a ChemClamp potentiostat and headstage (Dagan, Minneapolis, MN) with a two electrode system. The working electrode was either a CFME or a CNTYME, and the reference electrode was Ag/AgCl. To make an electrochemical connection between the electrode surface and the system, the capillary was filled with 1 M KCl. The dopamine waveform was applied (ramping from holding to switching potentials of −0.4 V to 1.3 V relative to reference Ag/AgCl; scan rate 400 V s^{-1}; repetition frequency 10 Hz), and the electrode was left to stabilize in PBS buffer until the background current was constant (5–10 minutes). A pre-treatment test was run to determine the electrode's response to the working solution (1 μM DA, EP, NE, 5HT; 20 μM DOPAC). After the electrode was treated in KOH, the same electrode was stabilized in PBS before measuring its response to the working solution. All solutions were injected from a syringe at 2 mL min^{-1} by a pump (Harvard Apparatus, Holliston, MA) and was facilitated with an air actuator (VIVI Valco Instruments, Houston, TX). Each trial was analyzed using HDCV Analysis program (Department of Chemistry, University of North Carolina at Chapel Hill).

Electrochemical treatments

The electrochemical treatment was applied using a Gamry Reference 600 potentiostat (Warminster, PA) and a three electrode system. The reference electrode was a Ag/AgCl reference electrode, the working electrode was either a CFME or a CNTYME, and the counter electrode was a platinum wire. All three electrodes were dipped in the 1 M KOH solution. For the CFMEs, a 1.5 V potential difference relative to the reference Ag/AgCl electrode was applied for 3 minutes. For the CNTYMEs, a 1.5 V potential was applied for 1 minute. After treatment, the electrode was then dipped in isopropanol for 5 seconds.

Surface characterization

Scanning electron microscopy (SEM) images were taken using an FEI Quanta 650 SEM (Thermo Fisher Scientific, Waltham, MA) to visualize the surfaces of a CFME and a CNTYME before treatment, after 1 minute of treatment, and after 3 minutes of treatment. X-ray photoelectron spectrometry (XPS) (Physical Electronics, Chanhassen, MN) was conducted to determine functional group and binding energies on the electrode surface. Al Kα monochromatic X-ray source (1486.6 eV) was used. Energies were obtained for CNTYME that were untreated, treated for 1 minute, and treated for 3 minutes. The C 1s peak was analyzed using MultiPak software to deconvolute the signal into the signals of sp^2-hybridized carbon (284.8 eV), sp^3-C (285.4 eV), C–O (287.0 eV), C=O (288.5 eV), and π–π* (290.0 eV). Raman spectroscopy was performed on a Renishaw InVia Confocal Raman microscope (Renishaw, Hoffman Estates, IL) to determine the surface defect sites. The D band occurs at 1360 cm^{-1} and the G band occurs at 1580 cm^{-1}. The ratio of the peaks was calculated by the intensity of the peaks.

Fouling and duration tests

Fouling test was performed by injecting a 1 μM serotonin–PBS solution for 5 seconds every 30 seconds, repeated 30 times. Cyclic voltammograms for the first and thirtieth injection were compared to determine fouling. Stability was determined by collecting a cyclic voltammogram every 0.5 hours for 4 hours at a CNTYME after KOH treatment.

Results and discussion

Surface characterization reveals fundamental differences between CFME and CNTYME

To understand how the treatment changes the electrode surfaces, SEM imaging was performed to visualize the surface area of the two electrodes, and then XPS and Raman spectra were performed to characterize the surface chemistry of a CNTYME.

To visualize how the KOH treatment changes the surfaces of CFMEs and CNTYMEs, SEM images were taken before and after KOH treatment of 1 and 3 minutes (Fig. 1). In Fig. 1A, the untreated CFME has a diameter of 7 μm and has grooves on the surface, which run parallel to the direction of the fiber

(Fig. 1A). In Fig. 1B, the CFME was treated for 1 minute in KOH with a 1.5 V potential difference applied, and the grooves become less pronounced. While the diameter has not significantly changed, the grooves become more shallow, so the electrode surface appears more smooth, which decreases the surface area. In Fig. 1C, the CFME was treated for 3 minutes in KOH with the same waveform applied. With this treatment, the diameter decreased from 7 μm to 5.9 μm, which decreased the surface area. Thus, KOH treatment smoothes the surface and decreases the surface area of a CFME.

Next, an untreated CNTYME (Fig. 1D) was compared to a CNTYME that was treated for 1 minute (Fig. 1E) or for 3 minutes (Fig. 1F) in KOH with a 1.5 V potential difference applied. In Fig. 1D, the untreated electrode appears relatively smooth, with some surface roughness on the left half. Polishing a CNTYME does not generate a perfectly smooth surface, which leaves some degree of surface roughness on an untreated CNTYME. In Fig. 1E, one minute of KOH treatment increased the surface roughness. More of the surface appears to have little spikes, and the peaks and valleys associated with these spikes increase both surface roughness and surface area. The white region in the bottom left is the epoxy seal. In Fig. 1F, the 3-minute treated CNTYME looks very different because the electrode developed major crevices on the surface. The cracks in the electrode occur because applying the 1.5 V potential difference for 3 minutes causes the individual CNTs to split apart from each other. The cracks in the surface dramatically increase the surface area, which caused background currents to increase so much so that the FSCV potentiostat's amplifier was saturated and the electrode could not be tested. Thus, treating a CNTYME at such a high potential in KOH for too long destabilizes the CNT yarn and causes the structure to fail. Consequently, the 1 minute treatment was used in the electrochemical tests to ensure the integrity of the carbon structure.

KOH treatment decreased the surface area of a CFME while it increased the surface area and surface roughness of a CNTYME. The changes in the CFME surface are a result of the 1.5 V potential breaking carbon–carbon bonds, decreasing striation, and shrinking the electrode diameter. The CFME was stable and the electrode maintained its structural integrity, so the 3 minutes treatment was used in electrochemical tests. A high potential breaks carbon–carbon bonds, which we propose is responsible for the etching.[13,16] Etching the CNTs generates surface roughness, and splitting individual CNTs exposes the walls of interior CNTs. Previous studies have shown that applying an anti-static gun can separate CNTs using charge, which is a similar result to the one observed here when a high potential is applied in a charged salt solution.[28]

XPS and Raman spectroscopy were then performed to characterize the surface chemistry of an untreated, a 1 minute KOH treated, and a 3 minutes KOH treated CNTYME. The total carbon 1s XPS signals for each CNTYME can be deconvoluted to show contributions from bonds of sp^2-hybridized carbons (284.8 eV), sp^3-C (285.4 eV), C–O (287.0 eV), and C=O (288.5
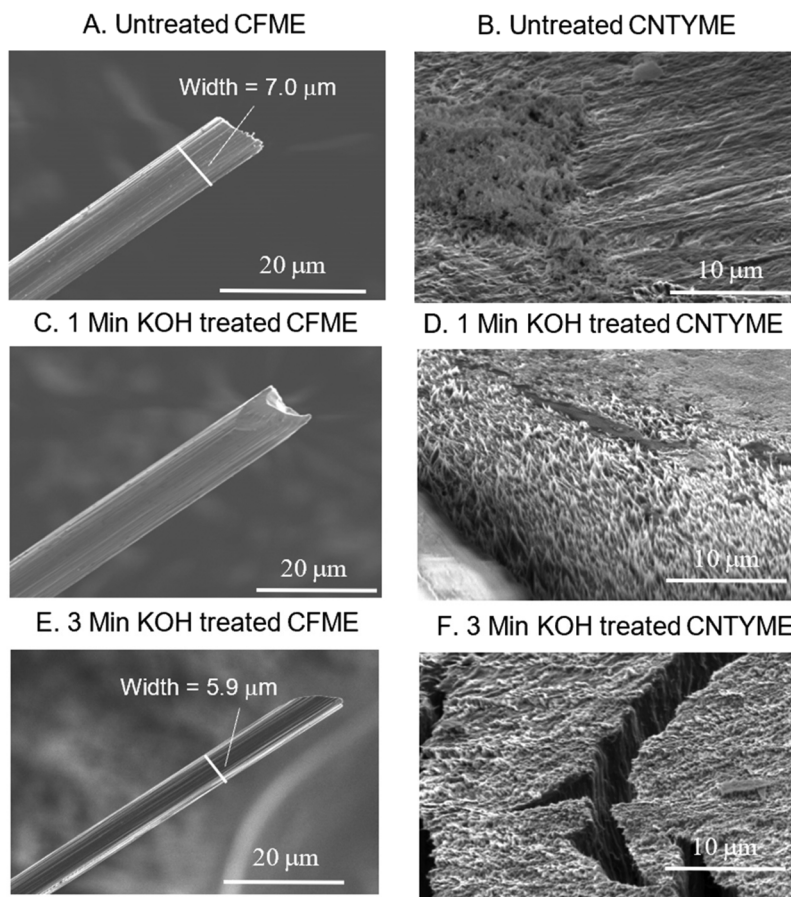
Fig. 1 Scanning Electron Microscopy (SEM) images of treated and untreated CFMEs and CNTYMEs. Left: CFMEs. (A) Untreated CFME, (B) 1 minute of KOH treatment, and (C) 3 minutes of KOH treatment. Right: CNTYMEs. (D) Untreated CNTYME, (E) 1 minute of KOH treatment, and (F) 3 minutes of treatment.

eV), and π–π* (290.0 eV) for some. Table 1 shows the relative abundances by area under each peak. The trend in the XPS data reveals that with longer treatment of CNTYMEs, the relative abundance of total carbon (sp^2 and sp^3) decreases while the relative abundance of oxygen–bound carbon (C–O and C=O) increases. An untreated CNT is mainly sp^2-hybridized carbon, with less sp^3 carbon at the edge plane or in oxygen functional groups. As the treatment is applied for longer periods of time, the 1.5 V potential breaks carbon–carbon bonds, and the amount of carbon–oxygen bonds (C–O or C=O) on the surface

increases from 20.4% to 38.3%. This indicates that this treatment breaks carbon–carbon bonds and increases the amount of oxygen functional groups on the surface.

Next, Raman spectra was performed to understand graphitic and defect peaks for an untreated CNTYME (Fig. 2D), a 1 minute- (Fig. 2E), and a 3 minutes- (Fig. 2F) KOH treated CNTYME. There are two characteristic peaks: a D band at 1360 cm^{-1} and a G band at 1580 cm^{-1}. The D band indicates the level of non-graphitic carbon, which can be identified as surface defect sites.[35] As the KOH treatment is applied for longer periods of time at the CNTYME, the ratio of the intensities of the D : G bands increases from 0.66 (untreated), 0.84 (1 minute), to 0.90 (3 minutes). The increasing trend in the ratio demonstrates that the treatment creates non sp^2-hybridized carbon. The XPS and Raman data together indicate that as KOH treatment is applied for more time, less graphitic carbon remains and more surface defect sites appear on the surface of the CNTYME.

Electrochemical treatment in KOH improves CFME and CNTYME performance

For the electrochemical tests, we first examined how KOH treatment affected CFMEs and their response to each neuro-

Table 1 Deconvoluted XPS C 1s peak for CNTYMEs

	Binding energy (eV)	Untreated (%)	1 min KOH (%)	3 min KOH (%)
sp^2 C	284.8	57.5	48.8	35.0
sp^3 C	285.4	16.9	22.8	20.5
Sum of sp^2 C and sp^3 C		74.4	71.6	55.5
C–O	287.0	12.4	23.4	25.9
C=O	288.5	8.0	0.9	12.4
Sum of C–O and C=O		20.4	24.3	38.3
π–π*	290.0	5.2	4.1	6.2
Total		100.0	100.0	100.0

Fig. 2 XPS and Raman data for surface characterization of treated and untreated CNTYMEs. Left: C 1s regions of the XPS data of a CNTYME that was (A) untreated, (B) after 1 minute of KOH treatment, and (C) after 3 minutes of KOH treatment. The total C 1s peaks are deconvoluted into sp²-hybridized carbon (284.8 eV), sp³-C (285.4 eV), C−O (287.0 eV), C═O (288.5 eV), and π−π* (290.0 eV). Right: Raman spectroscopy of a CNTYME that was (D) untreated, (E) after 1 minute KOH treatment, and (F) after 3 minutes of KOH treatment.

Fig. 3 FSCV results pre- and post-treatment for a CFME. Measurements were collected on a CFME pre- (black) and post- (red) treatment for (A) 1 µM DA, (B) 1 µM EP, (C) 1 µM NE, (D) 1 µM 5-HT, (E) 20 µM DOPAC, and for the (F) background.

transmitter. FSCV faradaic and background currents were collected before and after the KOH treatment for dopamine, epinephrine, norepinephrine, DOPAC, and serotonin (Fig. 3). The potential was held constant at 1.5 V *vs.* Ag/AgCl for 3 minutes while the electrode tip was submerged in 1 M KOH. After treatment, the current for each analyte increased between 1.5- and 2-fold, and the increase was very consistent for all the analytes, including all the cationic neurotransmitters and the negatively charged metabolite DOPAC. Although faradaic currents increased, the background currents decreased (Fig. 3). DA, NE, and 5-HT have similar CV shapes pre- and post-treatment, featuring an increase in the primary peak (Fig. 3). However, the treatment increases another oxidation peak of epinephrine at the switching potential,[25] and the primary oxidation peaks on epinephrine and DOPAC shift toward a lower potential (Fig. 3). Another interesting trend is that the pre- and post-treatment background currents have similar shapes, but the magnitude decreases after treatment (Fig. 3F). This decrease in background current is expected if the surface area decreases, as shown by the SEM. Paired *t*-tests were run to compare the current before and after treatment for each analyte (Fig. 4). There were significant increases of the faradaic current for
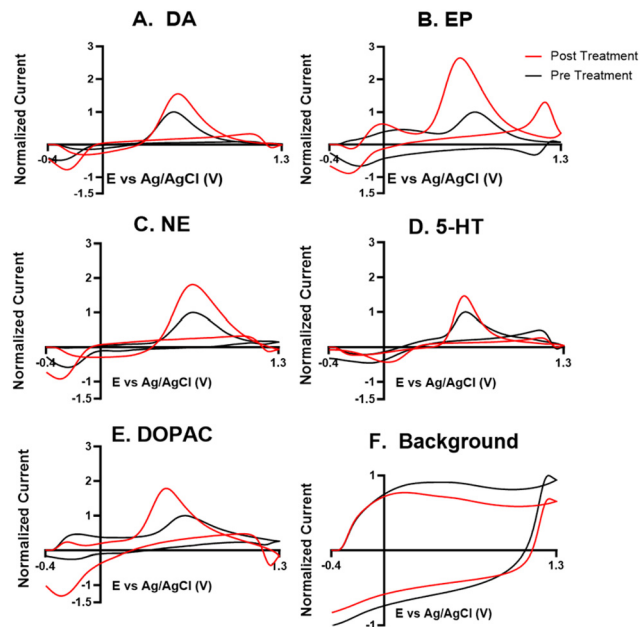
each analyte ($p < 0.05$ or $p < 0.01$) and a significant decrease in the background currents ($p < 0.001$).

Next, the KOH treatment was applied to CNTYMEs to understand their responses to each neurochemical. Here, the 1.5 V potential in KOH was applied for 1 minute to increase the surface area without cracking the electrode surface. In Fig. 5, the faradaic signal for each analyte increases between 2- and 4-fold, while the background also increases roughly 2-fold (Fig. 5). The CVs pre- and post-treatment for DA, NE, and 5-HT on a CNTYME have a similar shape to those on a CFME, but the CNTYME CVs feature a greater increase in the primary peak (Fig. 5). A secondary oxidation peak for EP increases as a shoulder at a lower potential than the primary peak.[25] CNTYME sensitivity to anions is improved with KOH treatment because the signal for DOPAC is increased roughly 2-fold. Paired *t*-tests were run to compare the faradaic and background currents of each analyte before and after treatment (Fig. 6). There were significant increases in faradaic currents for all five analytes ($p < 0.05$ or $p < 0.01$) and a significant increase in the background ($p < 0.0001$). Fig. S1A–E† shows calibration curves for all of the analytes, and the sensitivity for each analyte was improved by as much as 3.5-fold. Stability was also tested for dopamine, and the KOH-treated CNTYME had the same signal for dopamine when it was measured every 30 minutes for 4 hours (Fig. S1F†). Thus, these data demonstrate that CNTYMEs has increased sensitivity for each neurotransmitter.

A difference between CFMEs and CNTYMEs is that the CFME background currents decreased while the CNTYME background increased roughly two-fold with KOH treatment
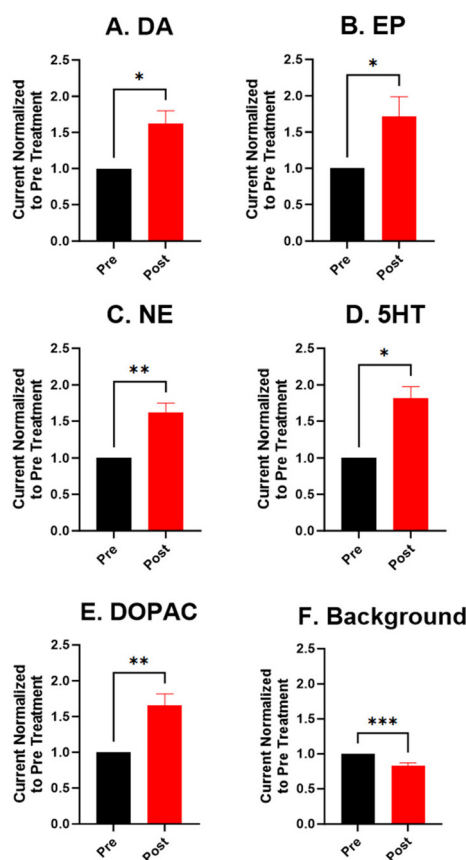
Fig. 4 Statistics on current pre- and post-KOH treatment for each neurotransmitter on a CFME. Paired *t*-tests were performed for each analyte, normalized to pre-treatment (1), *n* = 6. (A) 1 μM DA ($p < 0.05$), (B) 1 μM EP ($p < 0.05$), (C) 1 μM NE ($p < 0.01$), (D) 1 μM 5-HT ($p < 0.05$), (E) 20 μM DOPAC ($p < 0.01$), and (F) background ($p < 0.001$).
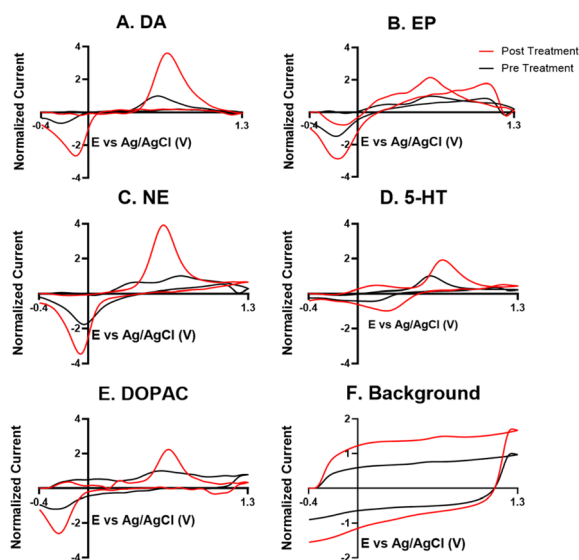

Fig. 5 FSCV results pre- and post-KOH treatment for a CNTYME. Measurements were collected on a CNTYME pre- (black) and post- (red) treatment for (A) 1 μM DA, (B) 1 μM EP, (C) 1 μM NE, (D) 1 μM 5-HT, (E) 20 μM DOPAC, and for the (F) background.
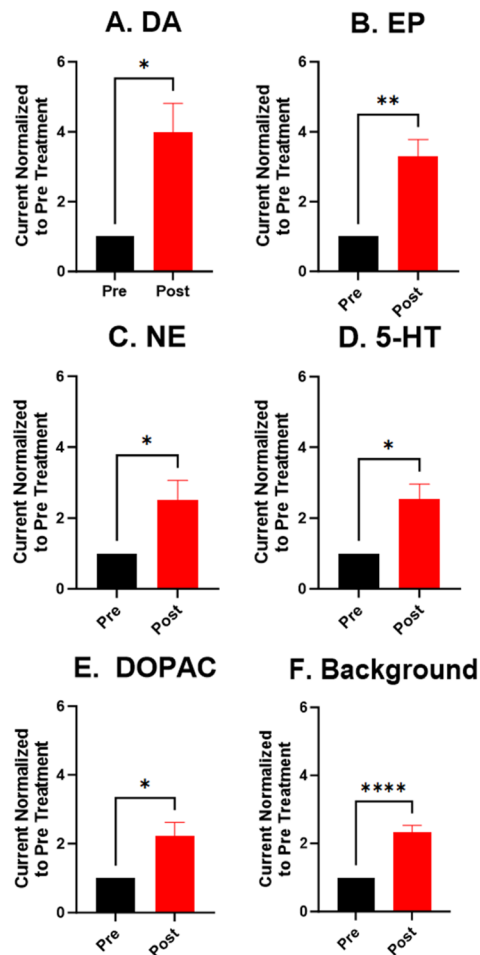

Fig. 6 Statistics on current pre- and post-KOH treatment for each neurochemical on a CNTYME. Paired *t*-tests were performed for each analyte, normalized to the pre-treatment (1), *n* = 5. (A) 1 μM DA ($p < 0.05$), (B) 1 μM EP ($p < 0.01$), (C) 1 μM NE ($p < 0.05$), (D) 1 μM 5-HT ($p < 0.05$), (E) 20 μM DOPAC ($p < 0.05$), and (F) background ($p < 0.0001$).

(Fig. 3F and 5F). The significant decrease of the CFME background current provides electrochemical support that the KOH treatment etches the carbon surface by breaking graphitic carbon–carbon bonds, which decreases CFME diameter and surface roughness. However, the electrochemical data shows an increase in CFME sensitivity to each analyte, despite a decrease in surface area. The KOH treatment adds oxygen functional groups to the edge plane carbons which facilitates better analyte adsorption, so the treatment activates the electrode for the detection of each neurochemical. In contrast to the CFME, the CNTYMEs have a larger surface area because the etching separates CNTs and generates deeper pockets and cracks between individual CNTs on the disk electrode. The increase in CNTYME background current provides electrochemical support that KOH treatment increases surface area. There is also an increase in sensitivity to each neurochemical, indicating a similar electrode activation for the detection of these neurochemicals.

A strength of this KOH treatment is that it increases CFME and CNTYME sensitivity to a variety of types of analytes. The treatment of both electrodes increases response to dopamine, epinephrine, norepinephrine, and serotonin in a similar fashion, which indicates that the monoamines respond favorably to the treated electrodes. The KOH treatment increases sensitivity to epinephrine because there is more analyte adsorption, which makes the secondary oxidation peak more pronounced. The secondary peaks of EP are more pronounced for electrodes with high surface roughness because the analyte can be momentarily trapped inside the small pockets.[25,41,42] Thus, the KOH treatment enhances trapping by making the surface rough, which explains the increased secondary peak on the treated CNTYME. The enhanced secondary peak on epinephrine also proves that the treatment enhances selectivity from the structurally-similar norepinephrine. Also, CVs are more reversible for CNTYMEs after treatment, with more similar magnitude for the reduction peaks compared to the oxidation peaks, a feature previously seen at trapping electrodes with crevices.[9,42]

For DOPAC on the CNTYME, however, the increase of faradaic current is roughly equal to the increase of background current (Fig. 6). Thus, it is unlikely that changes in surface chemistry contribute as much as the increased surface area to the increased signal. Therefore, the KOH treatment does not activate the CNTYME as much for anions. The treatment separates the individual CNTs to create cracks on the surface, inside of which there are more adsorption sites.[41] However, anions may not diffuse into these small pockets nor adsorb to the surface because their negative charge will be repelled when the electrode is at a negative holding potential. It is also unclear whether DOPAC adsorbs as strongly to oxygen functional groups. Thus, a CFME is activated similarly for DOPAC and cations, but the activation of a CNTYME depends on the charge of the analyte.

KOH treatment reduces electrode fouling

Fouling is a common problem for carbon electrodes, caused when biomolecules or polymerized byproducts coat the electrode surface to block neurotransmitter adsorption sites.[16,36] Serotonin is known to cause electrode fouling because its electrooxidation creates side products which polymerize into a film on the electrode surface.[37] Remedies to fouling have been widely studied, and include new waveforms, electrode coatings, and electrochemical treatment.[16,38–40] To better understand how the KOH treatment improves the electrode's performance, repeated injections of serotonin were performed to assess fouling.

Fig. 7 compares fouling with 30 repeated injections of serotonin on an untreated CNTYME and a KOH-treated CNTYME. In the untreated CNTYME, the serotonin CV after the thirtieth injection is roughly the same shape as that after the first injection, but the magnitudes of the oxidation and reduction peaks are diminished. Thus, the untreated electrode experiences significant fouling, which indicates the CNTYME signal decreases over time after serotonin exposure. On the treated electrode, the CVs of the first and the thirtieth injections appear about the same shape, and the heights of the primary oxidation and reduction peaks are similar (Fig. 7B). The secondary oxidation peak decreases, but not as much as it did on the untreated electrode. Compared to a KOH-treated CNTYME, there is significantly more fouling on the untreated electrode (Fig. 7C; unpaired t-test, $p < 0.001$, $n = 4$). Thus, the KOH treatment adds oxide groups, which lead to antifouling properties for serotonin.

Both surface area and surface chemistry contribute to the increased electrode performance to the four monoamines. Background current increases proportionally with surface area, which means more analyte molecules will fit on the larger CNTYME surface. But because the faradaic current increased more than 2-fold while the background increased only 2-fold, then a larger surface area is not the only factor involved in improving the signal. For this reason, the electrode is activated to cations because the surface chemistry changes also increase electrode sensitivity. The increase of oxygen on the surface shown by the XPS and Raman data will facilitate better cation adsorption, and it will reduce fouling. Surface oxygen may interfere with π–π stacking of the sp²-hybridized carbon at the edge and disrupt the adhesion of fouling products. Thus, the 1-minte KOH treatment boosts sensitivity and limits fouling.

In summary, the KOH treatment increases sensitivity for each neurochemical at both CFMEs and CNTYMEs, but has different mechanisms for the increases. It etches the CFME to decrease surface area, yet it activates the surface to increase
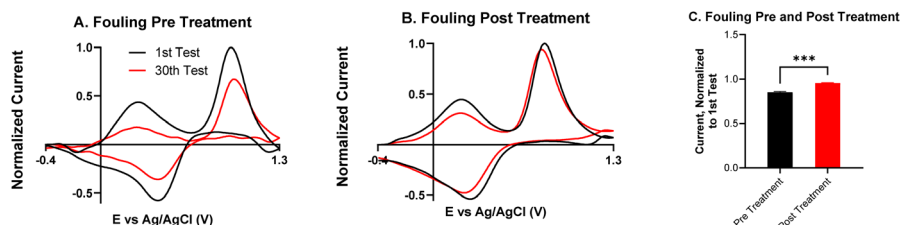

Fig. 7 Electrode fouling measurements at an untreated and a KOH treated CNTYME. 1 μM 5-HT was injected for 5 seconds every 30 seconds, repeated 30 times. (A) CVs from an untreated CNTYME show a decrease on the 30th injection. (B) CVs from a 1-minute KOH treated CNTYME show the signal is largely preserved on the 30th injection. (C) Unpaired t-tests compare the 1st and 30th signal ($p < 0.001$, $n = 4$) and there was a significant difference in the fouling.

signal by 1.5-fold. For the CNTYME, the signal increase is larger for cations and the background increases because of a larger surface area caused by pockets between individual CNTs. Thus, KOH treatment is particularly advantageous for CNTYMEs and increases the sensitivity to a variety of analytes.

Conclusions

In this work, we explored how two different carbon materials, CFMEs and CNTYMEs, respond to dopamine, epinephrine, norepinephrine, DOPAC, and serotonin after undergoing a KOH treatment, and we found that both electrodes have increased sensitivity to each neurochemical. The CFME has an activated surface with more oxygen, but that surface actually has smaller area due to etching. While the CNTYME cracks with longer times of etching in KOH, a 1-minute etch time increases the surface area and activates the surface to allow for improved neurotransmitter detection. This treatment is quick, easy, and inexpensive, so it should be a standard step used in the fabrication of both of these electrodes. KOH-treated CFME and CNTYME are important for improving real time, *in vivo* detection of neuroactive chemicals, so as understanding of the brain develops, better electrodes will improve understanding of the relationship between brain chemistry, behavior, and neural biology.[43,44]

Author contributions

Samuel M. Hanser – investigation, writing original draft, formal analysis, project administration. Zijun Shao – methodology, software, resource. He Zhao – data collection. B. J. Venton – supervision, review & editing, validation, funding acquisition.

Conflicts of interest

There are no conflicts to declare.

Acknowledgements

References

1 B. J. Venton and Q. Cao, Fundamentals of Fast-Scan Cyclic Voltammetry for Dopamine Detection, *Analyst*, 2020, **145**, 1158–1168, DOI: **10.1039/C9AN01586H**.

2 J. E. Baur, E. W. Kristensen, L. J. May, D. J. Wiedemann and R. M. Wightman, Fast-Scan Voltammetry of Biogenic Amines, *Anal. Chem.*, 1988, **60**(13), 1268–1272.

3 B. M. Kile, P. L. Walsh, Z. A. McElligott, E. S. Bucher, T. S. Guillot, A. Salahpour, M. G. Caron and R. M. Wightman, Optimizing the Temporal Resolution of Fast-Scan Cyclic Voltammetry, *ACS Chem. Neurosci.*, 2012, **3**(4), 285–292, DOI: **10.1021/cn200119u**.

4 R. M. Wightman, C. Amatore, R. C. Engstrom, P. D. Hale, E. W. Kristensen, W. G. Kuhr and L. J. May, Real-Time Characterization of Dopamine Overflow and Uptake in the Rat Striatum, *Neuroscience*, 1988, **25**(2), 513–523.

5 R. L. McCreery, Advanced Carbon Electrode Materials for Molecular Electrochemistry, *Chem. Rev.*, 2008, **108**(7), 2646–2687, DOI: **10.1021/cr068076m**.

6 N. T. Rodeberg, S. G. Sandberg, J. A. Johnson, P. E. M. Phillips and R. M. Wightman, Hitchhiker's Guide to Voltammetry: Acute and Chronic Electrodes for in Vivo Fast-Scan Cyclic Voltammetry, *ACS Chem. Neurosci.*, 2017, **8**(2), 221–234, DOI: **10.1021/acschemneuro.6b00393**.

7 C. G. Eleftheriou, J. B. Zimmermann, H. D. Kjeldsen, M. David-Pur, Y. Hanein and E. Sernagor, Carbon Nanotube Electrodes for Retinal Implants: A Study of Structural and Functional Integration over Time, *Biomaterials*, 2017, **112**, 108–121, DOI: **10.1016/j.biomaterials.2016.10.018**.

8 M. L. A. V. Heien, P. E. M. Phillips, G. D. Stuber, A. T. Seipel and R. M. Wightman, Overoxidation of Carbon-Fiber Microelectrodes Enhances Dopamine Adsorption and Increases Sensitivity, *Analyst*, 2003, **128**, 1413–1419, DOI: **10.1039/b307024g**.

9 B. D. Bath, D. J. Michael, B. J. Trafton, J. D. Joseph, P. L. Runnels and R. M. Wightman, Subsecond Adsorption and Desorption of Dopamine at Carbon-Fiber Microelectrodes, *Anal. Chem.*, 2000, **72**(24), 5994–6002, DOI: **10.1021/ac000849y**.

10 B. D. Bath, H. B. Martin, R. M. Wightman and M. R. Anderson, Dopamine Adsorption at Surface Modified Carbon-Fiber Electrodes, *Langmuir*, 2001, **17**(22), 7032–7039, DOI: **10.1021/la0106844**.

11 D. Raju, A. Mendoza, P. Wonnenberg, S. Mohanaraj, M. Sarbanes, C. Truong and A. G. Zestos, Polymer Modified Carbon Fiber-Microelectrodes and Waveform Modifications Enhance Neurotransmitter Metabolite Detection, *Anal. Methods*, 2019, **11**(12), 1620–1630, DOI: **10.1039/c8ay02737d**.

12 J. G. Roberts, B. P. Moody, G. S. McCarty and L. A. Sombers, Specific Oxygen-Containing Functional Groups on the Carbon Surface Underlie an Enhanced Sensitivity to Dopamine at Electrochemically Pretreated Carbon Fiber Microelectrodes, *Langmuir*, 2010, **26**(11), 9116–9122, DOI: **10.1021/la9048924**.

13 P. Takmakov, M. K. Zachek, R. B. Keithley, P. L. Walsh, C. Donley, G. S. McCarty and R. M. Wightman, Carbon Microelectrodes with a Renewable Surface, *Anal. Chem.*, 2010, **82**(5), 2020–2028, DOI: **10.1021/ac902753x**.

14 M. Poon and R. L. McCreery, In Situ Laser Activation of Glassy Carbon Electrodes, *Anal. Chem.*, 1986, **58**(13), 2745–2750, DOI: **10.1021/ac00003a001**.

15 A. M. Strand and B. J. Venton, Flame Etching Enhances the Sensitivity of Carbon-Fiber Microelectrodes, *Anal. Chem.*, 2008, **80**(10), 3708–3715, DOI: **10.1021/ac8001275**.

16 Q. Cao, J. Lucktong, Z. Shao, Y. Chang and B. J. Venton, Electrochemical Treatment in KOH Renews and Activates Carbon Fiber Microelectrode Surfaces, *Anal. Bioanal. Chem.*, 2021, **413**(27), 6737–6746, DOI: **10.1007/s00216-021-03539-6**.

17 A. C. Schmidt, X. Wang, Y. Zhu and L. A. Sombers, Carbon Nanotube Yarn Electrodes for Enhanced Detection of Neurotransmitter Dynamics in Live Brain Tissue, *ACS Nano*, 2013, **7**(9), 7864–7873, DOI: **10.1021/nn402857u**.

18 C. B. Jacobs, I. N. Ivanov, M. D. Nguyen, A. G. Zestos and B. J. Venton, High Temporal Resolution Measurements of Dopamine with Carbon Nanotube Yarn Microelectrodes, *Anal. Chem.*, 2014, **86**(12), 5721–5727, DOI: **10.1021/ac404050t**.

19 L. Xiang, P. Yu, J. Hao, M. Zhang, L. Zhu, L. Dai and L. Mao, Vertically Aligned Carbon Nanotube-Sheathed Carbon Fibers as Pristine Microelectrodes for Selective Monitoring of Ascorbate in Vivo, *Anal. Chem.*, 2014, **86**(8), 3909–3914, DOI: **10.1021/ac404232h**.

20 J. J. Gooding, Nanostructuring Electrodes with Carbon Nanotubes: A Review on Electrochemistry and Applications for Sensing, *Electrochim. Acta*, 2005, **50**(15), 3049–3060, DOI: **10.1016/j.electacta.2004.08.052**.

21 C. E. Banks, T. J. Davies, G. G. Wildgoose and R. G. Compton, Electrocatalysis at Graphite and Carbon Nanotube Modified Electrodes: Edge-Plane Sites and Tube Ends Are the Reactive Sites, *Chem. Commun.*, 2005, 829–841, DOI: **10.1039/b413177k**.

22 K. Wang, H. A. Fishman, H. Dai and J. S. Harris, Neural Stimulation with a Carbon Nanotube Microelectrode Array, *Nano Lett.*, 2006, **6**(9), 2043–2048, DOI: **10.1021/nl061241t**.

23 A. Mendoza, T. Asrat, F. Liu, P. Wonnenberg and A. G. Zestos, Carbon Nanotube Yarn Microelectrodes Promote High Temporal Measurements of Serotonin Using Fast Scan Cyclic Voltammetry, *Sensors*, 2020, **20**(4), 1173, DOI: **10.3390/s20041173**.

24 W. Harreither, R. Trouillon, P. Poulin, W. Neri, A. G. Ewing and G. Safina, Carbon Nanotube Fiber Microelectrodes Show a Higher Resistance to Dopamine Fouling, *Anal. Chem.*, 2013, **85**(15), 7447–7453, DOI: **10.1021/ac401399s**.

25 Z. Shao, P. Puthongkham, K. K. Hu, R. Jia, M. V. Mirkin and B. J. Venton, Thin Layer Cell Behavior of CNT Yarn and Cavity Carbon Nanopipette Electrodes: Effect on Catecholamine Detection, *Electrochim. Acta*, 2020, **361**, 137032, DOI: **10.1016/j.electacta.2020.137032**.

26 I. Dumitrescu, P. R. Unwin and J. V. Macpherson, Electrochemistry at Carbon Nanotubes: Perspective and Issues, *Chem. Commun.*, 2009, 6886–6901, DOI: **10.1039/b909734a**.

27 C. Yang, E. Trikantzopoulos, M. D. Nguyen, C. B. Jacobs, Y. Wang, M. Mahjouri-Samani, I. N. Ivanov and B. J. Venton, Laser Treated Carbon Nanotube Yarn Microelectrodes for Rapid and Sensitive Detection of Dopamine in Vivo, *ACS Sens.*, 2016, **1**(5), 508–515, DOI: **10.1021/acssensors.6b00021**.

28 C. Yang, Y. Wang, C. B. Jacobs, I. N. Ivanov and B. J. Venton, O_2 Plasma Etching and Antistatic Gun Surface Modifications for CNT Yarn Microelectrode Improve Sensitivity and Antifouling Properties, *Anal. Chem.*, 2017, **89**(10), 5605–5611, DOI: **10.1021/acs.analchem.7b00785**.

29 T. G. Strein and A. G. Ewing, In Situ Laser Activation of Carbon Fiber Microdisk Electrodes, *Anal. Chem.*, 1991, **63**(3), 194–198, DOI: **10.1021/ac00003a001**.

30 Y. Li and A. E. Ross, Plasma-Treated Carbon-Fiber Microelectrodes for Improved Purine Detection with Fast-Scan Cyclic Voltammetry, *Analyst*, 2020, **145**(3), 805–815, DOI: **10.1039/c9an01636h**.

31 L. V. Kalia and A. E. Lang, Parkinson's Disease, *Lancet*, 2015, **386**, 896–912, DOI: **10.1016/S0140-6736(14)61393-3**.

32 J. D. Berke and S. E. Hyman, Addiction, Dopamine, and the Molecular Mechanisms of Memory, *Neuron*, 2000, **25**(3), 515–532, DOI: **10.1016/S0896-6273(00)81056-9**.

33 P. Hashemi, E. C. Dankoski, J. Petrovic, R. B. Keithley and R. M. Wightman, Voltammetric Detection of 5-Hydroxytryptamine Release in the Rat Brain, *Anal. Chem.*, 2009, **81**(22), 9462–9471, DOI: **10.1021/ac9018846**.

34 K.-P. Lesch and J. Waider, Serotonin in the Modulation of Neural Plasticity and Networks: Implications for Neurodevelopmental Disorders, *Neuron*, 2012, **76**(1), 175–191, DOI: **10.1016/j.neuron.2012.09.013**.

35 A. C. Ferrari and J. Robertson, Resonant Raman Spectroscopy of Disordered, Amorphous, and Diamondlike Carbon, *Phys. Rev. B: Condens. Matter Mater. Phys.*, 2001, **64**(7), 075414, DOI: **10.1103/PhysRevB.64.075414**.

36 Y. S. Singh, L. E. Sawarynski, P. D. Dabiri, W. R. Choi and A. M. Andrews, Head-to-Head Comparisons of Carbon Fiber Microelectrode Coatings for Sensitive and Selective Neurotransmitter Detection by Voltammetry, *Anal. Chem.*, 2011, **83**(17), 6658–6666, DOI: **10.1021/ac2011729**.

37 P. Hashemi, E. C. Dankoski, J. Petrovic, R. B. Keithley and R. M. Wightman, Voltammetric Detection of 5-Hydroxytryptamine Release in the Rat Brain, *Anal. Chem.*, 2009, **81**(22), 9462–9471, DOI: **10.1021/ac9018846**.

38 K. E. Dunham and B. J. Venton, Improving Serotonin Fast-Scan Cyclic Voltammetry Detection: New Waveforms to Reduce Electrode Fouling, *Analyst*, 2020, **145**(22), 7437–7446, DOI: **10.1039/D0AN01406K**.

39 I. Banerjee, R. C. Pangule and R. S. Kane, Antifouling Coatings: Recent Developments in the Design of Surfaces That Prevent Fouling by Proteins, Bacteria, and Marine Organisms, *Adv. Mater.*, 2011, **23**(6), 690–718, DOI: **10.1002/adma.201001215**.

40 X. Liu, T. Xiao, F. Wu, M. Y. Shen, M. Zhang, H. H. Yu and L. Mao, Ultrathin Cell-Membrane-Mimic Phosphorylcholine Polymer Film Coating Enables Large Improvements for In Vivo Electrochemical Detection, *Angew. Chem., Int. Ed.*, 2017, **56**(39), 11802–11806, DOI: **10.1002/anie.201705900**.

41 Z. Shao and B. J. Venton, Different Electrochemical Behavior of Cationic Dopamine from Anionic Ascorbic Acid and DOPAC at CNT Yarn Microelectrodes, *J. Electrochem. Soc.*, 2022, **169**, 026506, DOI: **10.1149/1945-7111/ac4d67**.

42 C. Yang, E. Trikantzopoulos, C. B. Jacobs and B. J. Venton, Evaluation of Carbon Nanotube Fiber Microelectrodes for Neurotransmitter Detection: Correlation of Electrochemical Performance and Surface Properties, *Anal. Chim. Acta*, 2017, **965**, 1–8.

43 B. J. Venton and R. M. Wightman, Psychoanalytical Electrochemistry: Dopamine and Behavior, *Anal. Chem.*, 2003, **75**(19), 414 A–421 A, DOI: **10.1021/ac031421c**.

44 P. Hashemi, E. C. Dankoski, R. Lama, K. M. Wood, P. Takmakov and R. M. Wightman, Brain Dopamine and Serotonin Differ in Regulation and Its Consequences, *Proc. Natl. Acad. Sci. U. S. A.*, 2012, **109**(29), 11510–11515, DOI: **10.1073/pnas.1201547109**.